

AD-A082 450

HUGHES RESEARCH LABS MALIBU CA

F/6 20/6

INFRARED FIBER OPTICS.(U)

DEC 79 J A HARRINGTON, R TURK, M HENDERSON

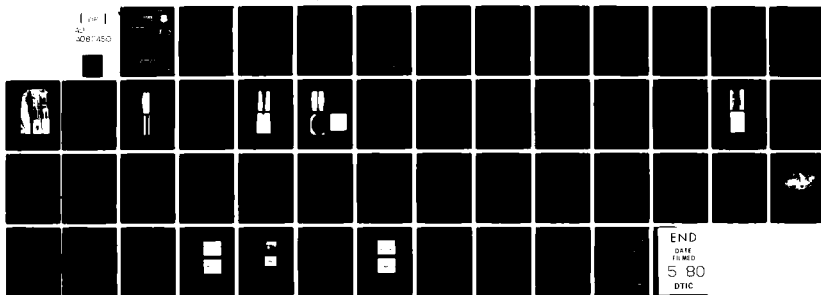
F19628-78-C-0109

UNCLASSIFIED

RADC-TR-79-290

NL

[1 of 1]
AD-A082 450



END
DATE
FILMED
5 80
DTIC

UNCLASSIFIED

SECURITY CLASSIFICATION OF THIS PAGE (When Data Entered)

19 REPORT DOCUMENTATION PAGE		READ INSTRUCTIONS BEFORE COMPLETING FORM	
18 1. REPORT NUMBER RADC-TR-79-290	2. GOVT ACCESSION NO.	3. RECIPIENT'S CATALOG NUMBER	
6 4. TITLE (and Subtitle) INFRARED FIBER OPTICS.	9 5. TYPE OF REPORT & PERIOD COVERED Interim Report 14 Apr 78 - 14 Apr 79	6. PERFORMING ORG. REPORT NUMBER N/A	
10 7. AUTHOR(s) J.A. Harrington M. Henderson R. Turk Jon Myer	15 8. CONTRACT OR GRANT NUMBER(s) F19628-78-C-0109 new		
9. PERFORMING ORGANIZATION NAME AND ADDRESS Hughes Research Laboratories 3011 Malibu Canyon Road Malibu CA 90265	16 10. PROGRAM ELEMENT PROJECT TASK AREA & WORK UNIT NUMBERS 61102F 2300130	17 11. REPORT DATE Dec 1979	
11. CONTROLLING OFFICE NAME AND ADDRESS Deputy for Electronic Technology (RADC/ESM) Hanscom AFB MA 01731	12 12. NUMBER OF PAGES 51	13. SECURITY CLASS. (of this report) UNCLASSIFIED	
14. MONITORING AGENCY NAME & ADDRESS (if different from Controlling Office) Same	15. DECLASSIFICATION/DOWNGRADING SCHEDULE N/A		
16. DISTRIBUTION STATEMENT (of this Report) Approved for public release; distribution unlimited.			
17. DISTRIBUTION STATEMENT (of the abstract entered in Block 20, if different from Report)			
18. SUPPLEMENTARY NOTES RADC Project Engineer: Harold Posen (RADC/ESM)			
19. KEY WORDS (Continue on reverse side if necessary and identify by block number) Infrared fibers Fiber optics Infrared materials IFF			
20. ABSTRACT (Continue on reverse side if necessary and identify by block number) This interim technical report summarizes the first year's research efforts to fabricate optical communications fibers that are transmissive between 1 and 12 μ m. The ultimate objective of this program is to prepare infrared transmitting fibers with losses less than 5 dB/km. In preparing infrared transparent fibers with these losses, we are emphasizing the extrusion into fiber of very pure KCl as this material has demonstrated bulk losses equal to or less than 5 dB/km in the 2- to 6- μ m region. The primary approach (Cont'd)			

DD FORM 1 JAN 73 1473

UNCLASSIFIED

SECURITY CLASSIFICATION OF THIS PAGE (When Data Entered)

172600

Jm

UNCLASSIFIED

SECURITY CLASSIFICATION OF THIS PAGE(When Data Entered)

Item 20 (Cont'd)

M. CROMBIEP S

used to meet the program goals, therefore, was the extrusion of reactive atmosphere process (RAP) grown KCl into 250- to 1000- μ m-diameter optical fibers. After one year of effort, the best KCl fiber extruded had a loss of 4200 dB/km.

The exceptionally high losses ($\sim 10^3$ times greater than the program goal) are primarily due to the poor surface quality of the KCl fibers. Our attempts at extruding better quality fiber have centered on two specific approaches. The first, and most common, is to use a lubricant to reduce friction between the extruded fiber and the diamond die. The second approach is to extrude at higher temperatures where the KCl can be extruded with lower friction without a lubricant. So far neither method has yielded a KCl fiber with a glassy-looking surface, such as produced, for example, by extruding KRS-5. Therefore, the observed losses are most probably not dominated by fundamental loss mechanisms but rather are due to scattering from gross surface irregularities.

This report also summarizes our efforts in fabricating a special infrared fiber prototype device for the detection of pulsed CO₂ laser radiation. This prototype device, which is to be used in a battlefield identification friend or foe (BIFF) application, was successfully field tested in Germany.

UNCLASSIFIED

SECURITY CLASSIFICATION OF THIS PAGE(When Data Entered)

TABLE OF CONTENTS

Section		Page
	PREFACE	5
1	INTRODUCTION AND SUMMARY	7
	A. Fiber Fabrication	8
	B. Evaluation	8
	C. BIFF	9
2	TECHNICAL PROGRESS AND DISCUSSION	11
	A. Fiber Fabrication	11
	B. Evaluation	24
	C. BIFF	39
3	FUTURE PLANS	49
	A. Task 1 - Fiber Fabrication	49
	B. Task 2 - Evaluation	49
	C. Task 3 - BIFF	49
4	PAPERS AND PRESENTATIONS	51

Accession For

NTIS GRA&I ☒

DDC TAB ☐

Unannounced

Justification

By

Dist. Division

Acquisition Code

Dist. Division

Special

A

PREFACE

This interim technical report describes work on infrared fiber optics performed during the period 14 April 1978 to 14 April 1979. The program manager is James A. Harrington, and the principal investigator is Anthony L. Gentile. Overall program coordination was provided by Morris Braunstein and Douglas A. Pinnow.

This program has involved the efforts of the following personnel: Jon Myer and Arlee Standlee extruded the KCl fibers; R. Turk and Nelson Ramirez made the mechanical measurements, prepared the billets, and obtained the lubricants; M. Henderson and Jon Myer designed, fabricated, and field-tested the BIFF apparatus; and J. Harrington and B. Bobbs performed the optical evaluation studies.

SECTION 1

INTRODUCTION AND SUMMARY

This interim technical report summarizes the first year's research efforts to fabricate optical communications fibers that are transmissive between 1 and 12 μm . The ultimate objective of this program is to prepare infrared transmitting fibers with losses less than 5 dB/km. To prepare infrared transparent fibers with these losses, we decided to emphasize the extrusion into fiber of very pure KCl as this material has demonstrated bulk losses equal to or less than 5 dB/km in the 2- to 6- μm region. The primary approach used to meet the program goals, therefore, was the extrusion of reactive atmosphere process (RAP) grown KCl into 250- to 1000- μm -diameter optical fibers. After one year of effort, the best KCl fiber extruded had a loss of 4,200 dB/km.

In Section 2, which reviews our technical progress on KCl fibers, we attempt to carefully analyze the nature and source of the very high losses ($\sim 10^3$ times greater than the program goal) measured in the current KCl fibers. To summarize, these losses are primarily due to the poor surface quality of the KCl fibers. Our attempts at extruding better quality fiber have centered on two specific approaches. The first, and most common, is to use a lubricant to reduce friction between the extruded fiber and the diamond die. The second approach is to extrude at higher temperatures where the KCl can be extruded with lower friction without a lubricant. So far neither method has yielded a KCl fiber with a glassy-looking surface, such as is produced, for example, by extruding KRS-5. Therefore, the observed losses are most probably not dominated by fundamental loss mechanisms but rather are due to scattering from gross surface irregularities.

The research program carried out during the past year is organized into several related tasks:

- Fiber fabrication
- Evaluation
- BIFF (battlefield identification friend or foe).

Fiber fabrication involves both extruding KCl fibers and also preparing the starting billet used in the extrusion. The billets are then usually coated with a lubricant for extrusion. Evaluation encompasses all of the optical and mechanical testing along with microscopic analysis of the fiber's polycrystalline structure. Finally, BIFF is a task devoted to fabricating a special infrared fiber prototype device for detecting pulsed CO₂ laser radiation. Technical progress in these areas is summarized below.

A. FIBER FABRICATION

During the past year, 25 KCl extrusions were performed to attempt to improve the quality of the KCl fiber. We had recognized early in the program that unlubricated KCl billets could not be extruded into good-quality fiber at temperatures below 400°C. Therefore, a wide variety of lubricants were tried to reduce the friction between die and fiber and thus to improve surface quality. Selecting an appropriate lubricant was particularly difficult because the lubricant must wet the surface of the KCl at elevated temperatures (>200°C) and be removable after extrusion. This has limited the choice of lubricants to waxes (paraffin, beeswax), polyethylene mixtures (Parafilm M), and solid lubricants (anthracene, p-terphenyl). To date, the best lubricants have been Parafilm and beeswax. Using these materials to coat the KCl billets, KCl fiber has been extruded at temperatures below 350°C with relatively smooth (to the eye) surfaces in lengths of up to 2 m. This fiber yielded the lowest losses, 4,200 dB/km, even though the fiber's surface had many irregularities. The high-temperature extrusions without lubricants have only been carried out at a maximum temperature of 520°C. To date, the surfaces of these fibers have also been of poor quality although higher temperatures must be tried before final judgement is made on this approach.

B. EVALUATION

Optical and mechanical evaluation of the bulk, billet, and fiber material has been carried out on a selected basis. In general, all

fibers are optically evaluated at 10.6 μm unless the surface quality of the fiber is so poor that insertion loss measurements are not justified. The RAP-grown bulk KCl has also been evaluated calorimetrically at 10.6 μm , as have some billets cut from this material. We discovered that the billets generally had absorption coefficients about 10 times less than the fibers extruded from them.

The 10.6- μm insertion-loss measurements on KCl fibers yielded a wide range of attenuation coefficients. Our initial extruded KCl fiber had losses in excess of 20,000 dB/km. Currently, our best fiber, extruded using Parafilm lubricant, had a loss of 4,200 dB/km. Of particular interest is that the losses are not particularly dependent on whether the fiber is measured with or without the lubricant on the fiber surface. This is unexpected since the lubricants are fairly lossy at 10.6 μm . The probable explanation is that surface irregularities still dominate the losses although, in the future, removal of the lubricants is expected to be a significant factor in reducing fiber loss.

The mechanical evaluation was limited to a few selected strength tests. The strongest KCl fiber had a yield strength of about 1000 psi for an extrusion temperature of 280°C (Parafilm lubricant). Photomicrographs were taken of each fiber to study grain size and surface quality. Grain size varied between 50 and 200 μm . The surface quality, which is a most important property at this point in the program, varied from highly fish scaled (milky appearance) to glassy-looking for the lubricated fibers. Removal of the lubricants often revealed longitudinal striations ("die marks") and etching in HCl, while removing the striations revealed the microcrystalline structure of the fibers.

C. BIFF

During the last few months of the first year's effort, the Army requested that a prototype IR fiber device be fabricated for use as a detector/transmitter of pulsed, TEA-laser (10.6- μm) radiation. In this application, a pulsed (coded) CO_2 TEA laser is used as a source in troop training or BIFF exercises. The detection of this coded information at distances up to 3 km is accomplished using an IR fiber/detector assembly

(BIFF device). Specifically, two (~50-cm-long) 250- μ m-diameter KRS-5 (thallium bromide) fibers detect the laser radiation and then transmit the signals to two HgCdTe detectors for processing.

The present BIFF device has successfully undergone proof-of-concept testing in NATO field tests being conducted in Grafenwohr, Germany. Future Army or other DoD systems will involve more complex systems involving arrays of IR fibers for the passive detection of IR radiation. One such application, for which this device is a test model, involves the linkage of CO₂-laser signals impinging on an armored vehicle to a central detector array. In this use, IR fibers would be placed at strategic points on the exterior of the vehicle (such as a tank used in troop-training exercises or BIFF) to receive coded IR signals. The signal would then be transmitted for signal processing via the waveguide to a central cooled detector located in the benign interior of the vehicle. Thus, the IR fibers would serve as simple detectors (which, unlike pyroelectric or other conventional detectors, require no power to operate) for incoming signals. They would also transmit information from a hostile environment (exterior of the vehicle) to an environment in which a central detector may conveniently be linked to signal-processing equipment. In this way, IR fiber waveguides currently under development at HRL may be used to reduce system costs by minimizing the number of detectors while simultaneously providing a passive fiber link that is resistant to EMI and enemy intrusion.

SECTION 2

TECHNICAL PROGRESS AND DISCUSSION

A. FIBER FABRICATION

1. Extrusion Mechanics

Extrusion methods have been used for the past three years to successfully fabricate KRS-5 and TlBr fibers. Polycrystalline fibers of these Tl-containing salts were prepared with losses as low as 300 dB/km (KRS-5). In this program, whose goal is to prepare IR fibers with 5-dB/km losses, we decided to pursue the extrusion of KCl because KCl has measured losses that are considerably better than those of KRS-5.

The extrusion process has worked well for the Tl-containing salts, in part because of the easy plastic deformation of these materials. Harder materials like KCl, NaCl, and KBr have proven more difficult to extrude owing to the higher melting points of these materials. The higher melting points ($>700^{\circ}\text{C}$) mean greater friction between the diamond die and billet, which results in extruded fiber with many surface irregularities. Imperfections may also be introduced in the bulk of the fiber due to the large extrusion pressure and deformation. Such imperfections may be distributed impurities or compositional fluctuations. In the latter case, variations in concentrations of Br^- and I^- in KRS-5 would lead to a gradient index that could be detrimental to fiber performance. Distributed impurities contributing to optical absorption losses can be reduced by further purification of the mixed crystal and its constituents. Reduction of inhomogeneities, on the other hand, requires a better understanding and control of extrusion process parameters. A computer program is presently being assembled to provide an insight into the incompressible flow patterns of the extruding medium.

To extrude a fiber, the selected diamond die aperture is installed in the press. HRL-made or factory-purchased core-drilled or cylinder-ground billets are coated with lubricant (if desired) and inserted in the cylinder chamber. The cylinder is heated to the desired extrusion

temperature, and the piston is advanced until the desired extrusion pressure is reached, as shown by the force gauge. In some cases, the fibers are quenched by a stream of LN_2 gas as they exit the die. A photograph of the larger, Mark III press is shown in Figure 1.

During the first year of the program, several improvements were made in the extrusion apparatus. These improvements have led to better control of the extrusion-process parameters as well as to better facilities for preparing long lengths of fibers. Specifically, the large Mark III press was put on line and used to produce 200 m of good quality (better than 5 db/m) 250- μm -diameter KRS-5 fiber. The accessory fiber feed and take-up modules originally designed for the Mark II press fit this machine and were used in this run. The pressure indicator of the Mark III press was calibrated using the high-pressure phase transitions of potassium bromide and bismuth. To increase the versatility of this press, steps were taken to extend the operating temperature above the original 280°C maximum by including a new higher power heater (still on order) and the necessary protective water cooling circuits (complete).

The smaller, Mark II press, which was used for most of the extrusion runs, was equipped with a pressure indicator for better pressure control. The temperature range of this apparatus was also increased through the addition of protective water cooling circuitry. This modification has permitted extrusion temperatures of 520°C to be attained. In the next several months, this range will be further extended by adding a 1000-W heater coil.

During the past year, 25 KCl extrusion runs were made. These runs are listed in Table 1.

2. Extrusion Lubricants

Excellent results in extruding KRS-5 fibers with no lubrication (Figure 2) led us to try the same techniques with KCl. But since KCl, unlike KRS-5, does not provide its own lubrication, fibers emerge with surfaces overworked and torn by extreme friction, showing fish-scale cracking from portions stressed beyond their rupture strength (Figure 3).

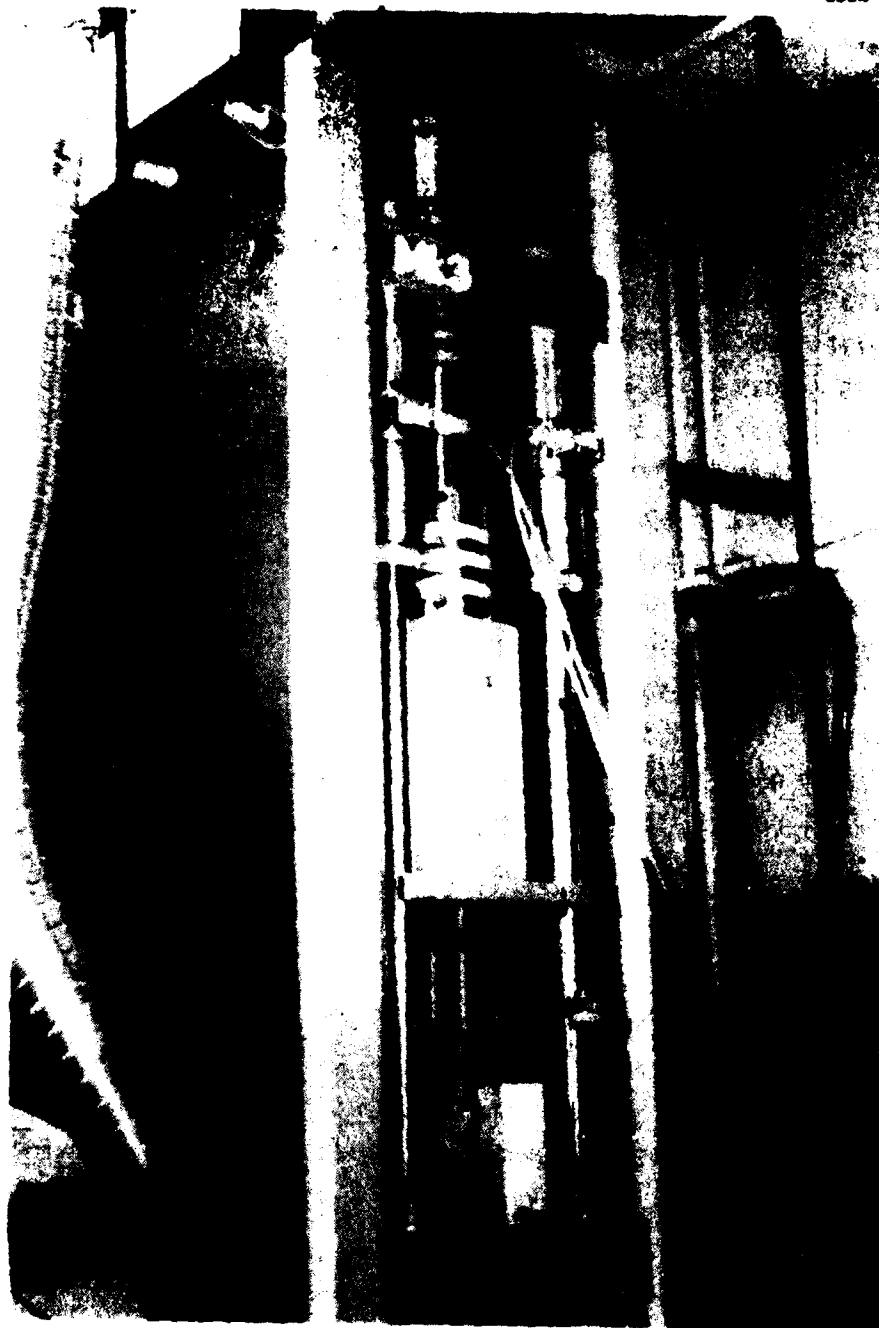


Figure 1. Mark III extrusion press for extrusion of long lengths (> 200 m) of 250- μ m-diameter fiber.

Table 1. KCl Extrusion Runs

Date	Run Number	Diameter, μm	Lube	Temperature, $^{\circ}\text{C}$	Force, kN
5/5/78	0008	300	None	385	
9/27/78	0019	250	MS-122	300-375	
10/5/78	0020	250	MS-122	300-325	
10/6/78	0021	250	None	310	
10/10/78	0022	250	None	310	
11/9/78	0025	250	None	330	
12/1/78	0027	250	None	350	
12/21/78	0028	1000	Crown wax	150	
12/22/78	0029	1000	None	175	
1/10/79	0031	1000	None	250	
1/16/79	0032	1000	None	280	
2/2/79	0035	1000	Parafilm	250	
2/14/79	0036	1000	Parafilm	200-280	
3/14/79	0039	500	Parafilm	200-300	4-6.5
4/17/79	0046	500	Parafilm	290	5-6
4/27/79	0048	500	Beeswax	250	5-12
5/4/79	0049	500	Beeswax-Montan	200-250	7-10
5/8/79	0050	500	Dekhotinsky	200	10-11
5/11/79	0053	500	Montan	200	11
5/14/79	0054	500	Cal Wax 180	200	
5/15/79	0055	500	Carnauba	200	14
5/16/79	0056	500	Anthracene	200	12
5/23/79	0059	500	None	525	3.5-5.5
5/23/79	0060	500	Vybar 103	100-225	7
5/30/79	0062	500	Grafoil	250	9.5

EXTRUSION WITHOUT LUBRICANT,
KRS-5 VERSUS KCl

8854-2

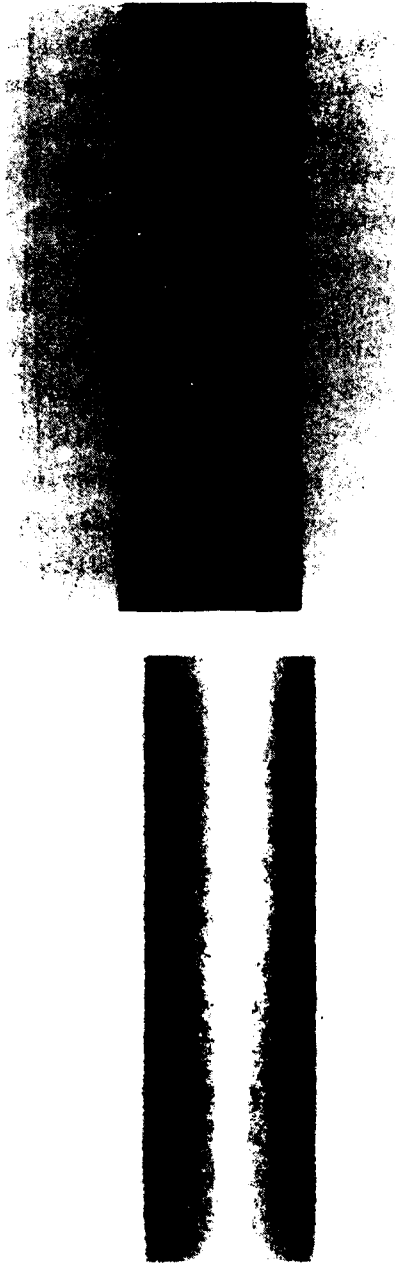


Figure 2. 100x, surface of KRS-5 extruded with no lubricant, 274 μ m diameter.

Figure 3. 100x, surface of KCl fiber extruded with no lubricant. Note torn fish-scale surface, 274 μ m diameter.

When the KCl billet is wrapped with a 0.005-in. layer of Parafilm lubricant prior to extrusion, an excellent surface results (Figures 4 and 5). This surface has longitudinal grooves typical of crystalline material drawn at high temperature. These are not "die marks" (the die is smooth), but result from uneven yielding of surface grains due to orientation differences. These grooves, which are the same size as internal grains, elongate into a fibrous structure during reduction. Drawn metal wires have this internal fibrous structure, but extruded KCl is equiaxed because it recrystallizes immediately after reduction.

The grooved surface can cause scattering and loss of transmitted power and thus should be removed. In KCl reduced from 5.5 mm to 1.0 mm (area reduction of 30:1), longitudinal surface grooves are 5 μ m deep (Figure 6). These disappear with a 30-sec etch in concentrated HCl, leaving a smooth surface with only grain boundaries visible (Figure 7). Longitudinal grooves in wire can be eliminated by drawing at room temperature, but the large reductions needed to make KCl fibers require pressures that preclude room-temperature extrusion with existing state-of-the-art tooling.

The cross section of a 30:1 extrusion is composed of large grains in a matrix of fine grains (Figure 8). The symmetrical arrangement results from a single-crystal extrusion billet whose longitudinal axis lies in the (100) plane but in a random direction.

The original crystal of KCl is fully polygonized and transformed into 20- μ m grains after the initial 100% area change, as in forging. These grains deform into elongated shapes as they pass through the die. On emerging, the deformed regions of highest energy recrystallize first, growing into larger grains with time at temperature, while less-deformed sections recrystallize into small grains. Thus, orientations of difficult slip have the most deformation energy and form the largest grains. With greater reductions, the additional distributed deformation causes growth of uniform large grains throughout the cross section.

The Parafilm lubricant is removed from the fiber by immersing the fiber in trichlorethylene for 20 min. This solvent does not attack the KCl surface. Striations and roughness are then removed by a 30-sec dip

EXTRUSION OF KCl WITH LUBRICANT AND
SIMILAR SURFACE BENEATH LUBRICANT

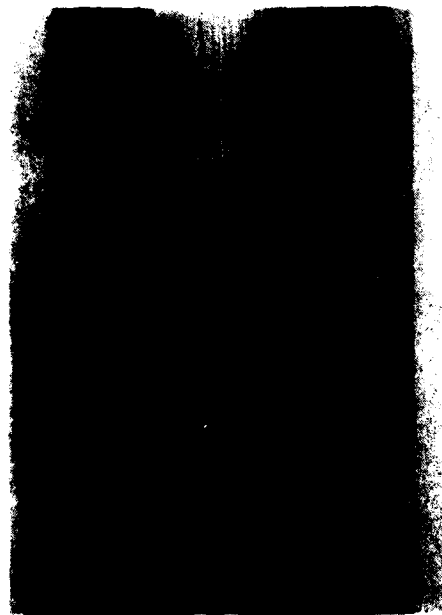


Figure 4. 100x, surface of KCl fiber
extruded with Parafilm
lubricant.

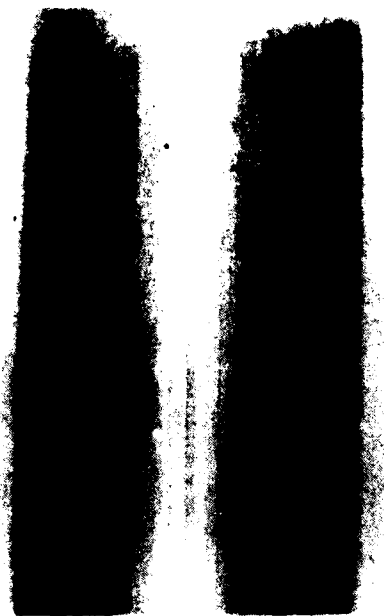


Figure 5. 100x, surface of extruded KCl
fiber with lubricant removed.

SURFACE GROOVES ON EXTRUDED KCl
AND
THEIR REMOVAL

8854-3



Figure 6. 100x, cross section of extruded KCl fiber after 30:1 reduction to 1.0 mm. Note surface grooves of 5 μ m depth.

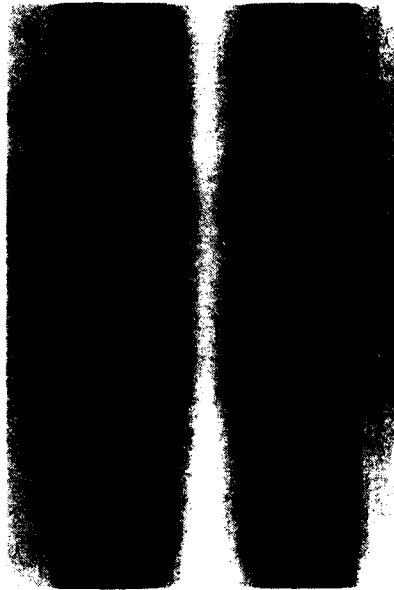


Figure 7. 100x, HCl-etched surface of extruded KCl fiber. Note disappearance of surface grooves and appearance of grain boundaries.



Figure 8. 66x, cross section of KCl fiber extruded at 30:1 to 1 mm diameter. Note symmetrical arrangement of large grains in a matrix of fine grains.

CROSS-SECTIONAL STRUCTURE OF EXTRUDED KCl

in HCl, leaving a surface that is highly polished with fine grain boundaries revealed (Figure 6). However, the polyethylene component of the lubricant has proven resistant to complete removal, preventing thorough etch-removal of extrusion grooves. Aromatic solvents have not been successful (xylene, toluene, benzene) nor has methylene chloride. A specific wax solvent, VM&P naphtha, will be tried when available. Also, we will try heated toluene and solvents to which surfactants have been added to improve wetting.

The successful extrusion of KCl fibers using Parafilm lube suggests that the most fruitful approach is to find a lubricant that be removed. The following lubricants were considered:

- Waxes
- Stearates
- Chemicals with foliated structure
- Greases
- Soaps
- Graphite foil
- Molybdenum disulfide
- Teflon.

Graphite, molybdenum disulfide, Teflon, and soaps are difficult to remove from the KCl surface without damaging the fiber. Nevertheless, graphite foil was tried as a lubricant, but it did not adhere to the billet surface during extrusion. Stearates and greases are only suitable below their melting points. The highest of these is zinc stearate which, at 130°C, is below our extrusion range of 140 to 300°C. Chemicals such as anthracene and para-terphenyl have suitable melting points and a foliated structure which should lubricate, but they do not adhere to the KCl surface during extrusion.

Even though all available waxes melt below 130°C, success with Parafilm led to additional wax lube experiments in the hope that a successful lube could be found that would be completely soluble.

Waxes are low-melting organic compounds of high molecular weight similar in composition to fats and oils but containing no glycerides.

Some are hydrocarbons, others are esters of fatty acids and alcohols. They are classed among the lipids. Waxes are thermoplastic but, since they are not high polymers, are not considered in the family of plastics. Major types are listed in Table 2. We have several waxes on hand, both natural and synthetic. These are listed in Table 3, along with other lubricant candidates. All of these waxes are applied by melting, with the preheated billet dipped into the molten wax.

At present, all KCl extrusions with lubricants other than Parafilm have been unsuccessful, with most of the melted wax extruded from the back of the extrusion die, leaving an unlubricated billet. Only the first 8 to 12 in. of fiber is lubricated, the remainder having a heavy fish scale surface. Extrusion runs are listed in Table 4.

Use of KRS-5 or TlBr as a lubricant for KCl is being considered, but we do not yet have an adequate way to apply it to the surface of the billet or to remove it afterward.

Ends of the fiber are ground and polished flat while mounted in a surrounding crystal of KCl. Chemical-mechanical polishing is used with 0.3 μ m alumina abrasive in a vehicle of propanediol on a cotton lap. This removes all worked surface (which absorbs infrared) and also reveals the grain structure of the cross section (Figure 8).

Table 2. Major Types of Waxes

Natural

Animal - beeswax, spermaceti, lanolin

Vegetable - carnauba, bayberry, sugar cane

Mineral - fossil (montan), petroleum (paraffin)

Synthetic

Ethylene polymers and polyol/ether-esters-sorbitol - carbowax

Chlorinated naphthalenes - Halowax

Hydrocarbon types

Table 3. Materials for Extrusion Lube

Material	Melting Point, °C +5°	Comments
Paraffin wax ^a	55	Petroleum derivative
Beeswax ^a	65	Vegetable derivative
Carnauba wax ^a	85	Vegetable derivative
Montan wax ^a	82	Mineral
Petrolite waxes:		
Polywax 2000	125	Synthetic ethylene homopolymer
C-1035	93	Microcrystalline
Vybar 103 ^a	72	Hydrocarbon polymer
EL020	117	Polyethylene
Amber 175	85	Microcrystalline, hard
C-400	104	Oxidized hydrocarbon
WB-14	-	Deriv. oxygenated H-C
Cal Wax 180 ^a	82	Microcrystalline, soft
Cal Wax 175	79	Microcrystalline, soft
DeKhotinsky wax ^a	-	
Anthracene ^a	216	Poor adherence
para-Terphenyl	212	
Grafoil ^a	-	Poor adherence
Parafilm ^a	-	Good lube, difficult removal
^a Tried as a lubricant for extrusion of KCl.		

Table 4. Lubricated KCl Extrusions of RAP Boule B154
at 120:1 (Final Diameter = 0.500 mm)

Run	T, °C	Lubricant	Surface	Grain Size μm	Yield Strength, psi
39	200	Parafilm	Good	110	823
	250	Parafilm	Good	196	1074
	280	Parafilm	Good	84	1015
	300	Parafilm	Good	70	715
	350	Parafilm	Good	128	823
46	290	Parafilm	Good		
48	250	Beeswax	Poor ^a		
49	200	Beeswax/Montan	Poor ^a		
50	200	Dekhotinsky	Poor ^a		
53	200	Montan	Poor ^a		
54	200	Calwax 180	Poor ^a		
55	200	Carnauba	Poor ^a		
56	200	Anthracene	Poor ^a		
59	525	No lube	Very poor		
60	200	Vybar 103	Poor ^a		
62	250	Grafoil	Poor ^a		
^a Initial 8 to 12 in. good					

B. EVALUATION

1. Mechanical Evaluation

The mechanical properties of the KCl fibers were studied by measuring the grain size, grain growth, and strength of selected KCl fibers. Since the emphasis in this program to date has been on optical properties, only limited data is available on the tensile strength of the fibers. Tensile strength was measured for five extruded KCl fibers, all of which were extremely brittle in flexure. Results are listed in Table 4. These yield strengths approximate that of single-crystal RAP KCl, indicating that grain growth has occurred following extrusion, with a subsequent drop in strength.

We have found that room-temperature grain growth in worked KCl is caused by a moist atmosphere with over 42% relative humidity.¹ This was qualitatively confirmed by tests on extruded fibers where polished surfaces were etched to reveal grain structure, exposed to moisture for 24 hr, and then re-etched to show growth of grains (Figures 9 and 10). These results show that extruded KCl must be protected from moisture after reduction, either with protective coating (lube) or in a dry atmosphere. The absorption of water will also increase IR absorption, so should be avoided.

A plot of extrusion temperature versus tensile yield strength (Figure 11) shows a maximum at 250°C, but the effect of time and atmospheric moisture on both grain size and tensile strength make any results questionable.

We believe that flexural ductility is of more importance than tensile strength during use and will direct efforts toward obtaining (and retaining) a fine-grained or fibrous structure to attain that goal.

¹"A New Mechanism to Inhibit Grain Growth in Forged KCl" R. Pastor et al., Proc. 5th Annual Conf. on Laser Window Matls., Dec. 1975, Las Vegas, Nevada, pg. 975, Defense Advanced Research Projects Agency.

EFFECT OF MOISTURE UPON GRAIN GROWTH,
EXTRUDED KCl FIBER

8854-4



Figure 9. 100x, longitudinal section of extruded KCl fiber. Note prevalence of fine grains.



Figure 10. 100x, same region as in Figure 9, re-etched after 24-hr exposure to moist atmosphere. Note exaggerated growth of grains.

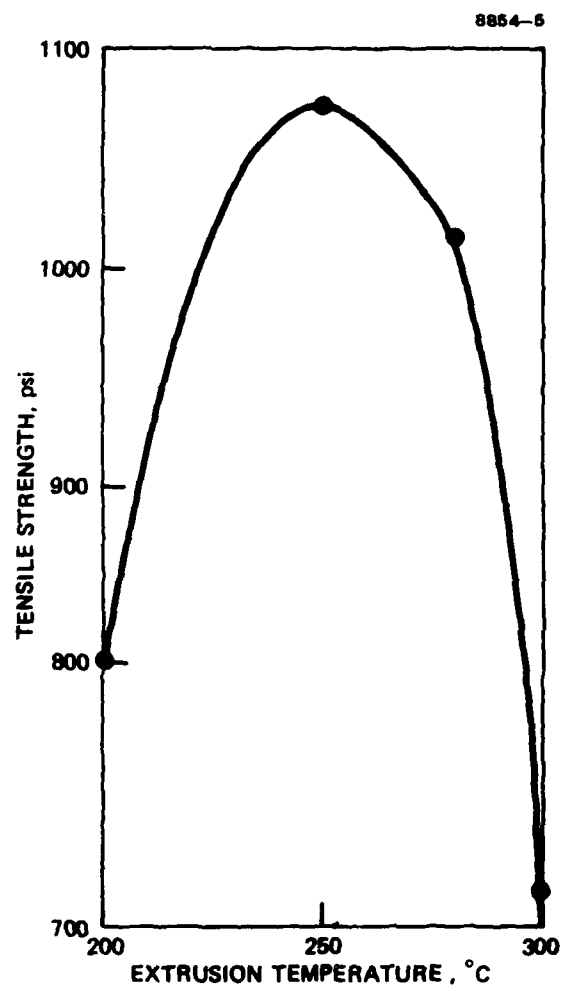


Figure 11. Extruded KCl fiber
tensile yield strength
versus extrusion
temperature.

2. Optical Evaluation

a. General Considerations

Two categories of optical evaluation were performed during the past year. The major portion of this effort was directed at making insertion-loss measurements on KCl fibers at 10.6 μm and evaluating the absorption coefficients in bulk and billet KCl material. The other area of investigation was the study of attenuation due to scattering. Here, a Brillouin light-scattering apparatus was established for measuring Rayleigh and Brillouin scattered light in transparent solids. By measuring the intensity of the scattered light it is possible to estimate the contribution that scattering makes to the total attenuation in low-loss materials.

b. Absorption Measurements

The material selected for extrusion was our RAP-grown, single-crystal KCl. This material provided high-quality, low-loss billets that have the potential of producing very transparent fiber. Before billet fabrication, the KCl windows were calorimetrically measured at 10.6 μm . Table 5 lists the results for the absorption coefficient β for seven different window samples. In some cases, older calorimetric data is also given so that current and past β 's can be compared to show the effect of aging. In general, the absorption is typical for RAP material, although lower values ($\sim 1 \times 10^{-4} \text{ cm}^{-1}$) have been obtained on some RAP crystals.

In the early stages of the program, 6-mm-diameter billets cut from the KCl windows listed in Table 5 were also evaluated calorimetrically at 10.6 μm . The absorption coefficients for the billets measured are given in Table 6.

Comparing these results with the absorption measured in the corresponding window indicates that the absorption is higher in the billets. This probably results from one of two sources. The major source suspected is the strong scattering present in the calorimetric

Table 5. 10.6- μm Absorption Coefficients for
KCl Windows

Sample No.	Thickness, cm	$\bar{\beta}$ (10.6 μm), cm^{-1}	Old $\bar{\beta}$ (10.6 μm), cm^{-1}
B155-2	1.30	$4.42 \pm 0.2 \times 10^{-4}$	0.88×10^{-4}
B155-6	1.11	$5.15 \pm 0.4 \times 10^{-4}$	--
B154-7	1.45	$3.94 \pm 0.1 \times 10^{-4}$	--
B154-3	1.38	$4.51 \pm 0.2 \times 10^{-4}$	--
B154-4	1.19	$6.41 \pm 0.3 \times 10^{-4}$	--
B59-DF-2	1.23	$4.17 \pm 0.1 \times 10^{-4}$	2×10^{-4}
B154-6	1.27	$4.34 \pm 0.4 \times 10^{-4}$	--

Table 6. 10.6- μm Absorption Coefficients for
RAP-Grown KCl Billets

Sample No.	Thickness, cm	$\bar{\beta}$ (10.6 μm), cm^{-1}
B155-6-1	3.74	8.14×10^{-3}
B155-6-2	3.86	3.72×10^{-3}
B154-7-1	4.72	2.17×10^{-3}
B155-2-1	3.58	9.65×10^{-3}

measurements for such small samples. Refinements in calorimetry (e.g., reduced scattering) led to the measurement of smaller β 's for the same sample, indicating that scattering is a probable source of error. The other possible source is the greater stress-induced birefringence in billets that results from cutting and grinding the billet to size. Further experiments to determine the relative contributions of these two sources or to further minimize this extraneous absorption were not pursued. This is because fibers extruded from these billets had losses typically 10 times greater than the billet loss, and we decided to direct more effort toward reducing fiber loss rather than trying to reduce the higher than expected billet losses.

The evaluation of fiber attenuation was made using a 10.6- μm CO_2 laser for insertion-loss measurements. The laser radiation was focused into the polished fiber end using a 1-in.-focal-length lens with an f-number typically near 4, although f-numbers between 2 and 8 were used with very little difference in the results. During the early stages of the program, most KCl was extruded with 1000- μm diameters so that the fiber could be more easily evaluated. More recently, this has been changed to 500- μm -diameter fiber as the extrusion of KCl improved.

The results in Table 7 are for the fibers extruded in the first part of the program. In two cases, data is presented for Rb^+ -doped KCl. This material was abandoned, however, after these two attempts so that more effort could be devoted to KCl.

Table 7. Fiber Losses at 10.6 μm for As-Extruded, Unlubricated KCl

Date	Diameter, μm	Sample No.	Sample	Loss, cm^{-1} (dB/m)
1/16/79	1000	B154-7-1	KCl	1.4×10^{-2} (6.09)
1/10/79	1000	B155-6-2	KCl	1.96×10^{-2} (8.52)
10/10/78	250	B156-1	KCl + Rb	4.05×10^{-2} (17.2)
12/22/78	1000	B156-2	KCl + Rb	2.06×10^{-2} (8.98)

Subsequent fiber extrusions below 350°C involved the use of a lubricant on the starting billet. The most successful lubricant was Parafilm. Table 8 gives the fiber loss data for the as-extruded, Parafilm-lubricated KCl and, in most cases, the results for the same fiber with the lubricant removed and after an HCl etch. Also indicated are the extrusion temperatures. The lowest losses occurred near the KCl recrystallization temperature of 280°C.

The most recent results are for fibers in which different lubricants were used. Since most of the fibers had poor-quality surfaces, optical evaluation was made on only a few of the best looking fibers. Table 9 summarizes the limited data on the lubricated fiber's best section. The Parafilm-lubricated fiber is listed in this table for comparison to the earlier results for the same lubricant given in Table 4. Unfortunately, the more recent run (No. 46) yielded a much poorer fiber than earlier runs (Nos. 36 and 39). The reason for this is not immediately understood, although it was noted that in run No. 46 the lubricant did not last as long as in the earlier runs. This implies that there may have been greater friction — and hence a poorer surface — in this case.

The most likely explanation for the high fiber losses is the fiber's poor surface quality. For the unlubricated KCl billets, excessive friction between the die and fiber resulted in a fish-scale surface that often appeared milky in cases of extreme friction. The losses in these fibers were excessive (essentially no transmission over a 25-cm length). The lubricated fibers also had surface irregularities, but not as severe as unlubricated ones. For these fibers, the longitudinal striations under the lubricant may have strongly scattered 10.6- μ m radiation. When these striations ("die marks") were removed by an HCl etch, after which the microstructure was revealed, the fibers were still lossy (see Table 8) even though there was no lubricant. In all cases, the surfaces were rough (with or without lubricant) and thus offered a means for radiation to be scattered out the sides of the fiber. In summary, we feel that if a smooth, clean-surface KCl fiber could be fabricated, the losses in KCl should be at least as good as they are for KRS-5 (10.6 μ m absorption, $7 \times 10^{-4} \text{ cm}^{-1}$ in the best material).

Table 8. Fiber Losses at 10.6 μm for Parafilm-Lubricated KCl Billets

Date	Run No.	Sample No.	Diameter, μm	Extrusion Temperature, $^{\circ}\text{C}$	As Extruded cm^{-1} (dB/m)	Lubricant Off cm^{-1} (dB/m)	HCl Etch, cm^{-1} (dB/m)
2/2/79	35	B154-7-2	1000	250	2.10×10^{-2} (9.0)	1.70×10^{-2} (7.43)	2.39×10^{-2} (10.4)
2/14/79	36	B154-7-3A	1000	280	1.50×10^{-2} (6.58)	1.50×10^{-2} (6.58)	2.01×10^{-2} (8.73)
		B154-7-3B	1000	200	2.97×10^{-2} (12.9)	1.88×10^{-2} (8.20)	1.88×10^{-2} (8.18)
3/14/79	39	B154-7-4A	500	200	6.53×10^{-2} (28.4)	--	2.71×10^{-2} (11.8)
		B154-7-4B	500	250	1.54×10^{-2} (6.71)	1.52×10^{-2} (6.59)	1.38×10^{-2} (5.99)
		B154-7-4C	500	280	1.16×10^{-2} (5.03)	--	0.96×10^{-2} (4.20)
		B154-7-4D	500	300	1.23×10^{-2} (5.33)	--	1.42×10^{-2} (6.18)
		B154-7-4E	500	350	5.43×10^{-2} (23.6)	--	4.72×10^{-2} (20.5)

Table 9. Fiber Losses at 10.6 μm for Various Lubricants
(Fiber Diameter of 500 μm)

Date	Sample No.	Run No.	Loss, cm^{-1} (dB/m)	Comment
4/17/79	B154-7-5	46	2.98×10^{-2} (13.0)	Parafilm, as extruded
5/23/79	B154-2-6	60	1.95×10^{-2} (8.46)	Vybar 103, as extruded
5/8/79	B154-7-8	50	5.8×10^{-2} (25.3)	Dekhotinsky, as extruded
			11.5×10^{-2} (49.9)	Dekhotinsky, removed

Another source of absorption is material losses. The data indicates, however, that the starting RAP-KCl is at least as good as KRS-5 at 10.6 μm , and, therefore, KCl fiber should, from a materials point-of-view, have bulk losses equal to or better than KRS-5 fiber. But this is not the case: KCl-fiber losses are usually 5 to 10 times those of KRS-5 fibers. Also based on our experience with hot, press-forged KCl laser windows, we know that KCl forged to 85% of its original length at temperatures between 250 and 350°C has a 10.6- μm absorption that does not differ appreciably from the single-crystal material. This suggests that the extruded KCl fiber material should be optically good and that, if the surfaces were comparable to KRS-5, the KCl fiber would have better transparency.

An interesting observation from Table 8 is that the lubricant does not seriously degrade the transmission of the KCl fiber. For Parafilm lubrication, removing the lubricant from the fiber improves the transmission by about 10 to 20%. This is somewhat surprising since Parafilm has strong absorption bands at 10.6 μm . These may be seen in Figure 12, which gives the infrared transmission spectrum of Parafilm M (thickness 0.005 in.). We feel that the reason that Parafilm or the other lubricants do not severely affect the transmission is that the fiber

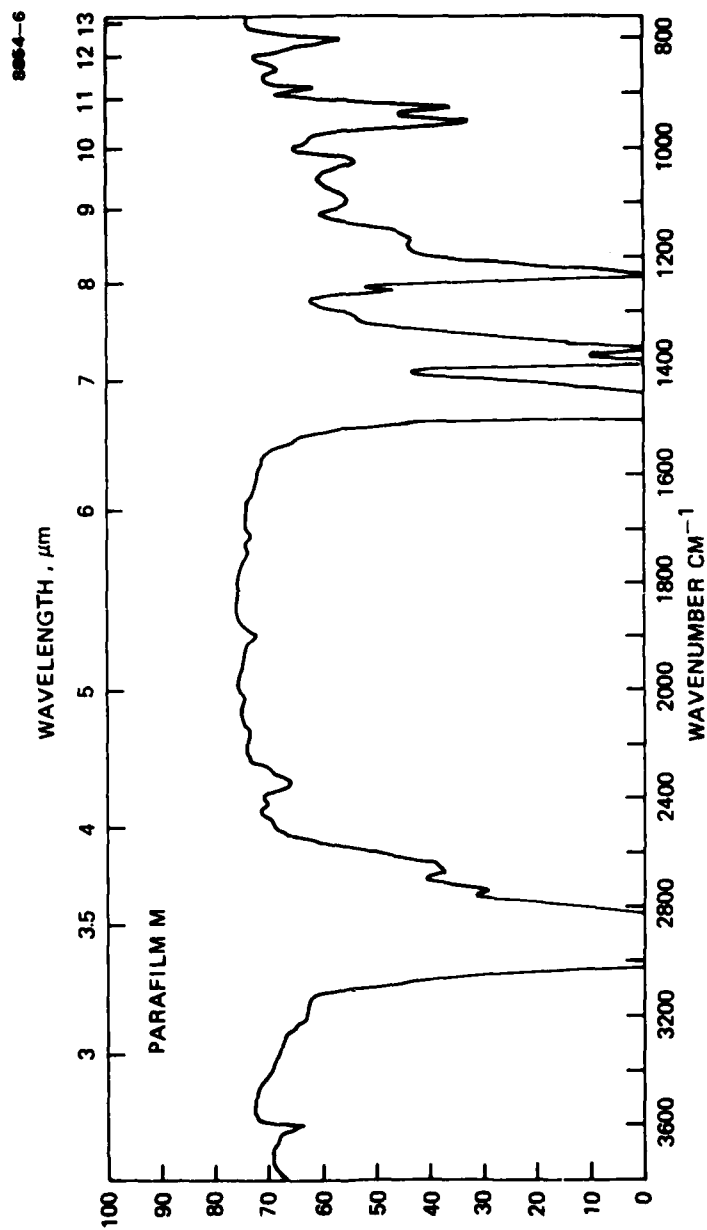


Figure 12. Infrared transmission of 0.005-in.-thick parafilm.

surfaces are so poor that scattering losses dominate any absorptive losses occurring in the lubricant "cladding." However, we suspected that, when KCl-fiber surfaces improve, losses in the lubricant will be a major source of the total attenuation. Therefore, we have selected lubricants that are readily soluble in common solvents that do not attack KCl. Early in the program we had thought that a lubricant could be found that would act as a cladding and thus be left on the fibers. But such a lubricant is not likely to be found because most organic materials are replete with absorption bands in this region or, in general, are not nearly as transparent as KCl. In addition the index of refraction of a lubricant/cladding must be less than 1.45. This also limits the choice of materials. Therefore, future lubricant studies will continue to be restricted to materials that can be removed from the fiber.

c. Scattering Measurements

The scattering studies are designed to determine the contribution of scattering to the total attenuation in transparent materials. In general, scattering and absorption are treated as independent effects and thus the total absorption coefficient β is the sum of scattering (β_s) and absorptive (β_a) processes:

$$\beta = \beta_s + \beta_a .$$

Our measurements of scattering will yield β_s , which, when coupled with the results for β_a (from Section 2.8.2.b), will provide a comprehensive account of the attenuation in low-loss materials.

The scattering measurements were made using a Burleigh Instruments DAS-System 3 Fabry-Perot (FP) interferometer. A schematic of the interferometer and associated optics and electronics is given in Figure 13. Brillouin and Rayleigh scattering spectra are recorded at 4820 and 5145 Å using an Ar⁺-laser source. The FP is actively stabilized

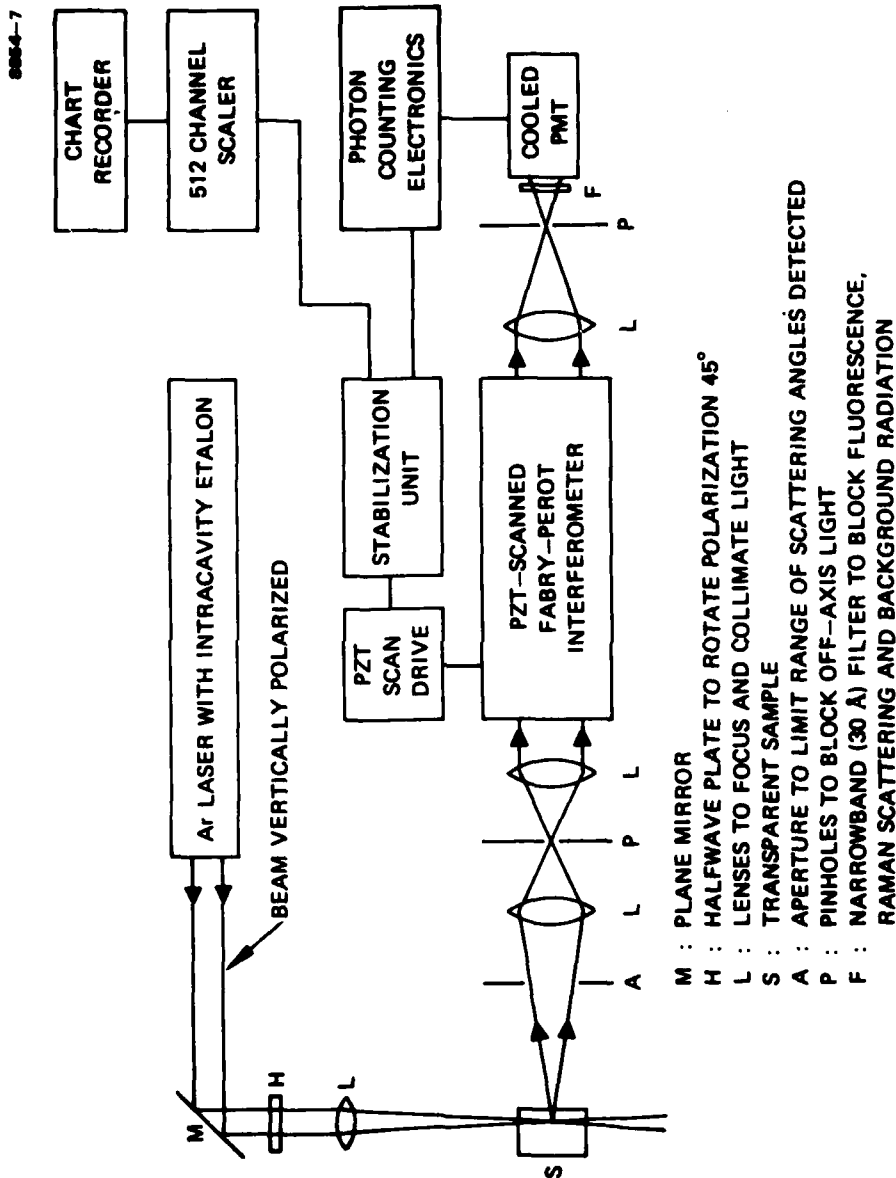


Figure 13. Burleigh Instruments DAS-System 3 Fabry-Perot interferometer.

against axial drift and mirror tilt (parallelism) so that repetitive scans are possible without loss of finesse. Instrument finesse in the single-pass mode of operation was measured to be approximately 60.

The scattering coefficient β_s is calculated in two steps. First, the ratio of the intensities of the Rayleigh-scattered light to the sum (Stokes plus anti-Stokes) of the Brillouin scattering components is measured. Their ratio, which is defined to be the Landau-Placzek ratio R_{lp} ,

$$R_{lp} = \frac{\text{Rayleigh intensity}}{\text{sum of Brillouin intensities}},$$

is used to calculate β_s from

$$\beta_s = \beta_B (R_{lp} + 1),$$

where β_B is the attenuation coefficient due to Brillouin scattering alone. The coefficient β_B is calculated from the basic materials properties.

As a calibration of our equipment, R_{LP} was first measured for fused SiO_2 . Figure 14 shows the scattering spectra for silica. Note the intense Rayleigh-scattered light characteristic of glasses. From this figure, R_{lp} is calculated to be 28. This falls within the range of 21 to 28 given by others for fused SiO_2 . The fact that this sample falls at the high end of the range indicates that this particular sample is a stronger scatterer of light than are most fused quartz samples.

In single-crystal material, Rayleigh scattering is theoretically very near zero. Thus, $R_{lp} \approx 0$, and β_s is expected to be quite small. Figure 15 shows the spectrum of single-crystal CaF_2 . Although less than for a glass (e.g., SiO_2), the Rayleigh scattering is still stronger than expected. The measured R_{lp} for this sample is 11, indicating

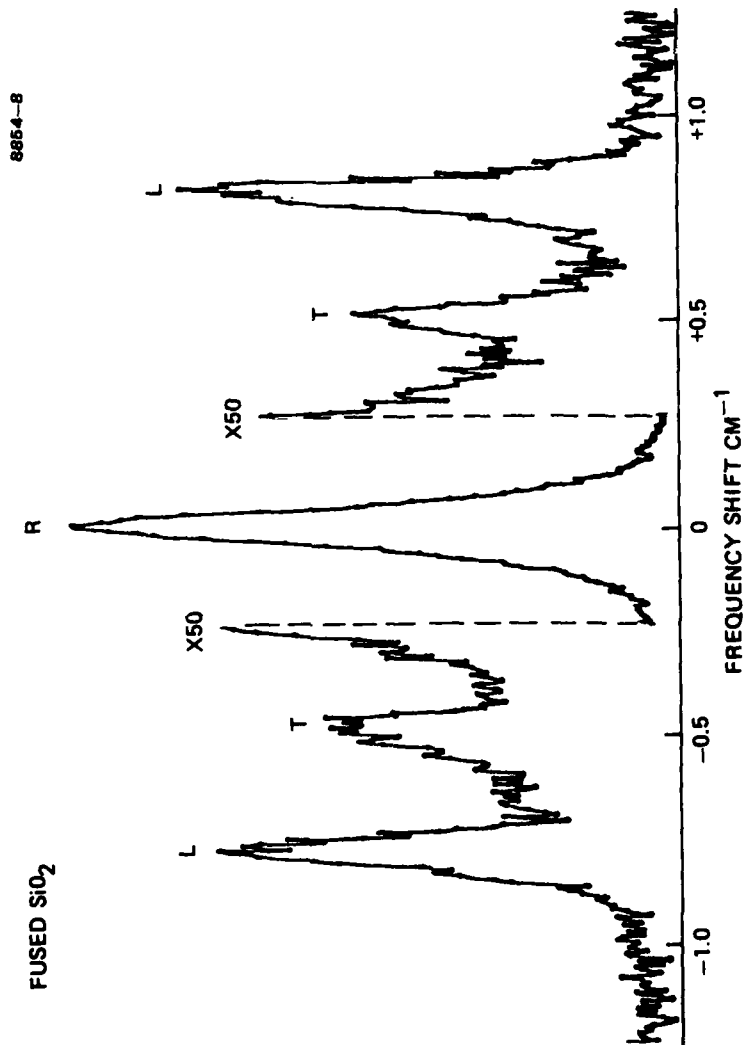


Figure 14. Scattered light spectrum (4880 \AA) of fused SiO_2 showing Rayleigh (R) and Brillouin (longitudinal L, transverse T) lines.

SINGLE CRYSTAL
 CaF_2

8854-9

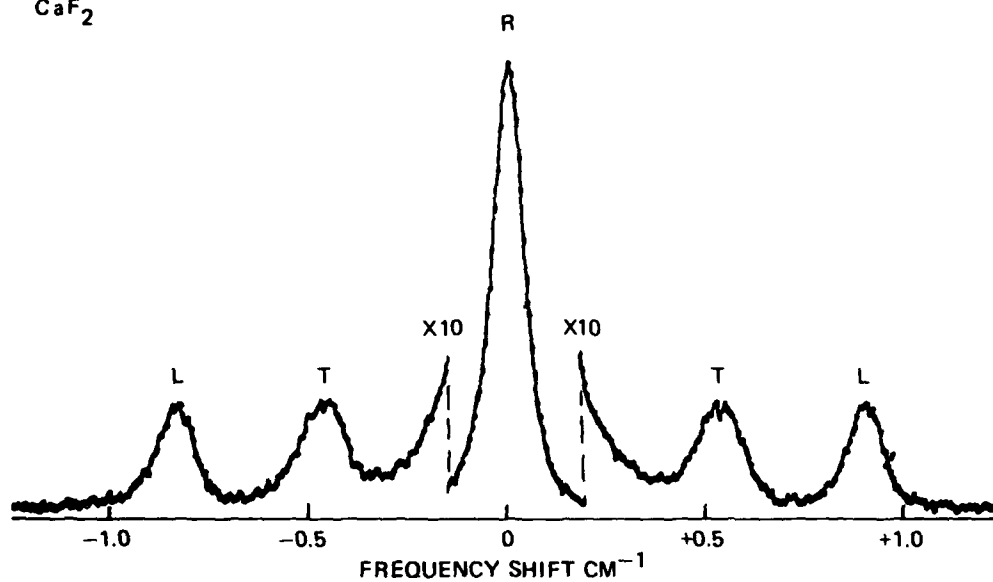


Figure 15. Scattered light spectrum (4880 \AA) of CaF_2 showing Rayleigh (R) and Brillouin (longitudinal L, transverse T) lines.

that the scattering is much higher than predicted. Further work is needed to determine the source of this strong scattering in this single-crystal material.

C. BIFF

Until early 1979, all our experience with IR fibers had been gained under laboratory conditions. There existed no knowledge of how these fibers would perform under the rugged conditions of field use. During May and June of this year, an IR fiber receiver fabricated by Hughes was used in NVEOL field tests of candidate battlefield-identification-friend-or-foe (BIFF) systems. The fibers and detectors performed flawlessly under extreme conditions of heat, dust, vibration, and humidity. Although these tests do not represent MIL-Spec testing of the fiber, the results are encouraging. This section describes the design, testing, and performance of this receiver system.

1. Receiver Design

A photograph of the IR fiber receiver is shown in Figure 16. The main elements of the unit consist of two flexible fiber cables, two HgCdTe detectors in dewars, and the supporting frame. A pointing scope used in aligning the receiver is also visible.

The fibers are 250- μ m-diameter, \sim 0.5-m-long KRS-5. The fibers are first sheathed in a small (0.075 in. i.d.) plastic tube. This unit is then placed in a larger plastic tube which mates with the fiber connectors. Commercial AMP connectors are used that allow the fiber cable to be replaced simply if needed. The fiber input ends are mounted on sliding posts (visible in the figure); this allows the fiber-to-fiber separation to be varied from 1 cm to 50 cm. This feature was included in the receiver design to permit the correlation lengths of received CO₂ laser pulses to be measured in the field tests.

HgCdTe detectors from Santa Barbara Research Center (SBRC #40742) were mounted to the frame. Each of these 2-mm-square detectors was

MC12913

FIBER CABLES

8854-10

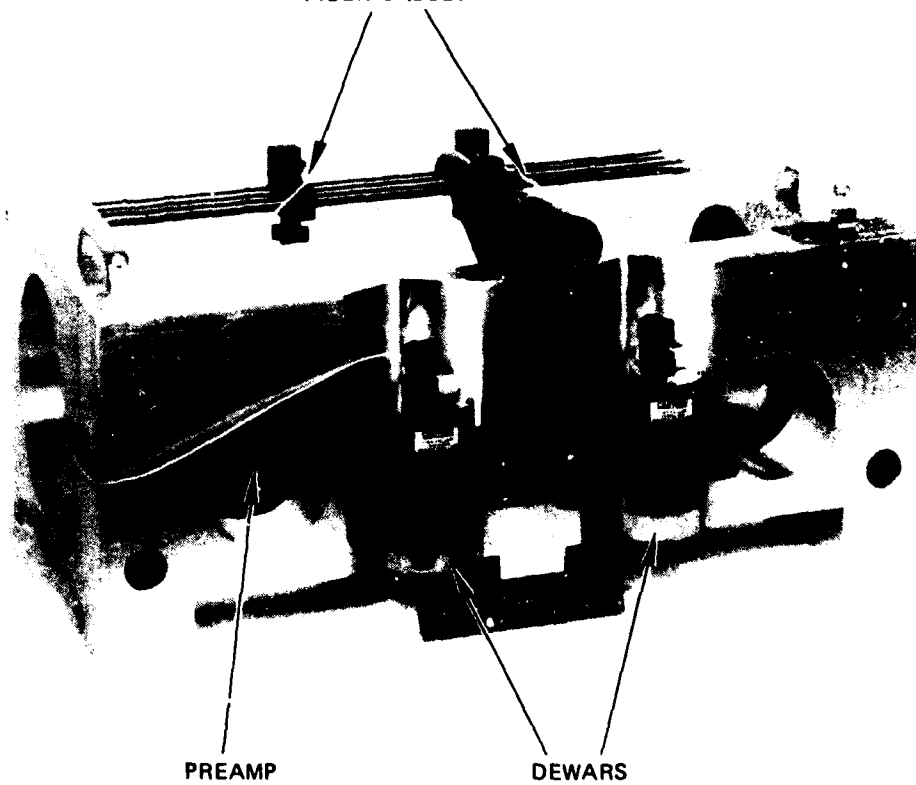


Figure 16. BIFF prototype device with two IR fibers for detection of pulsed-CO₂ laser radiation.

bonded to specially prepared cold fingers to locate the detector 1.5 mm from the inside surface of the Irtran II entrance window. The output fiber end was itself located 41 mm from the input side of the window. This close coupling and large detector area allowed all of the light captured by the fiber to irradiate the detector. Since the window was not AR coated, loss was high, ~30%. If necessary, this loss could be reduced by coating the window.

2. Performance

The receiver's performance was measured with the test setup shown in Figure 17. The attenuated output of a CO₂ laser, which was expanded with a lens, illuminated the fiber input. A removable bending mirror was used to calibrate the beam intensity I_{inc} by illuminating a Molelectron Pyroelectric Radiometer.

The power received by the detector, P_{rec} , is given by

$$P_{rec} = \tau_f \tau_w A_f I_{inc}, \quad (1)$$

where τ_f is the transmission of the fiber, τ_w is the transmission of the window, and A_f is the area of the fiber. The detector noise, expressed in noise-equivalent power (NEP), is

$$NEP = \frac{1}{D^*} (A_d \Delta f)^{\frac{1}{2}}, \quad (2)$$

where D^* is detector sensitivity, A_d is the area of the detector, and Δf is receiver bandwidth. The measured signal-to-noise ratio in the experiment is simply

$$\frac{S}{N} = \frac{P_{rec}}{NEP}, \quad (3)$$

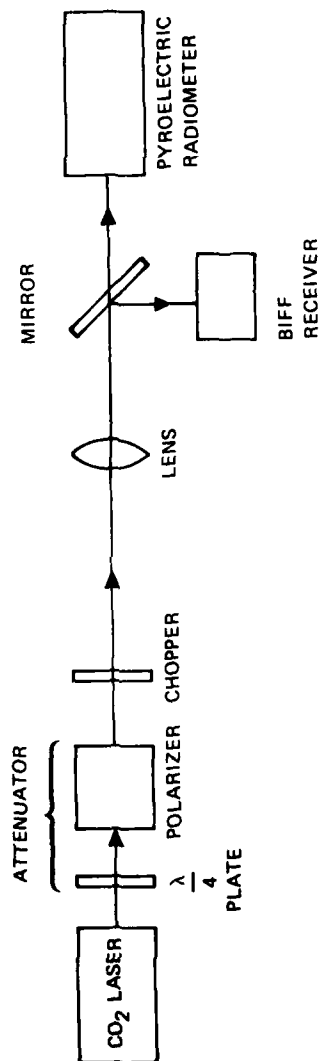


Figure 17. BIFF test set-up in our laboratory.

from which the detector D^* can be calculated:

$$D^* = \frac{(A_d \Delta f)^{1/2}}{\tau_f \tau_o I_{inc} A_f} \frac{S}{N} \quad (4)$$

The measured performance for the two detectors as shown in Figure 18 is for the following numerical values:

$$A_d = 0.2 \text{ cm} \times 0.2 \text{ cm}$$

$$\Delta f = 10 \text{ MHz}$$

$$\tau_f = 0.6$$

$$\tau_o = 0.7$$

$$I_{inc} = 800 \text{ } \mu\text{m}/\text{cm}^2$$

$$A_f = 5 \times 10^{-4} \text{ cm}^2 \text{ (250 } \mu\text{m diameter).}$$

The measured S/N for detector 3895 is 2:1 under these conditions, while it is 4:1 for detector 3896. The resulting values are

$$D^*(3895) = 7.4 \times 10^9 \text{ W}^{-1} \text{ Hz-cm}$$

$$D^*(3896) = 1.5 \times 10^{10} \text{ W}^{-1} \text{ Hz-cm.}$$

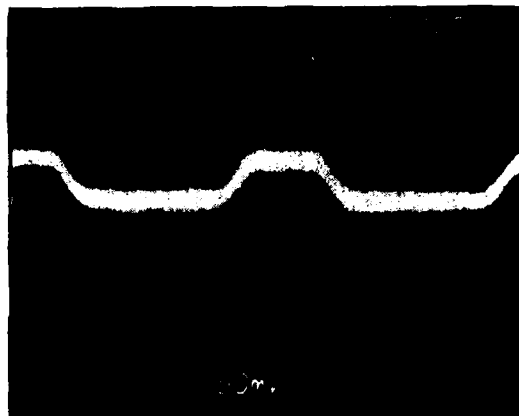
Thus, the detectors, which have a stated D^* of 1×10^{10} , are performing properly.

The measured fiber FOV was $\pm 30^\circ$, which is limited at present by the location of the recessed fiber in its housing. The fibers themselves have much larger acceptance angles.

The detector speed was tested by illuminating the fibers with greatly attenuated 150-nsec-wide TEA laser pulses. The recorded traces are shown in Figure 19. The pulse rises in ~ 125 nsec and is followed by

8854-12

DET NO. 3895



DET NO. 3896

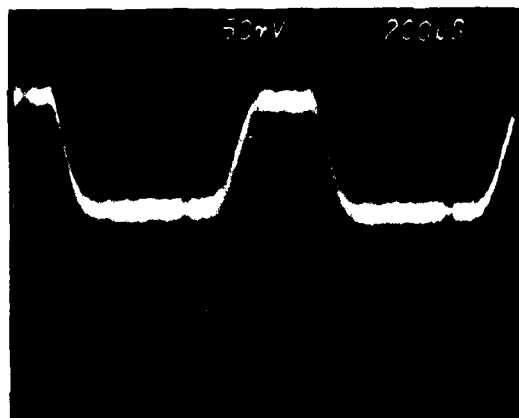
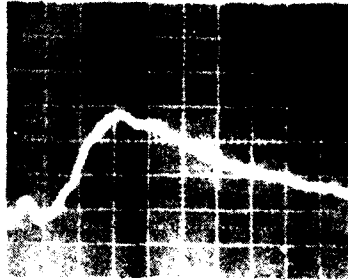


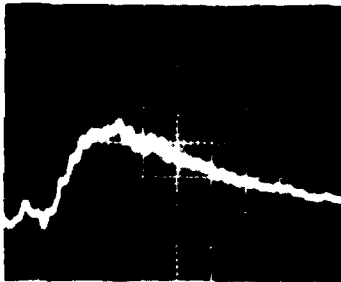
Figure 18. Measured response of two HgCdTe detectors used in BIFF prototype device.

8854-13

DET NO. 3895



DET NO. 3896



100 ns/DIV
200 mv/DIV

Figure 19. Response of HgCdTe detectors illuminated with TEA laser pulses.

a long diffusion tail. Faster HgCdTe detectors for resolving some of the structures of the pulse are available with an accompanying reduction in D^* . The pressures of meeting a short turnaround schedule precluded the selection of optimal detectors. It is important to realize that pulse resonance is a function of the material characteristics and not of the detector size. If we reduce the detector area to reduce capacitance, the chip resistance goes up in the same proportion and hence the RC time constant of the detector remains the same.

We recognized that an important part of the field test would be a simple on-site verification of fiber continuity. Thus, a prototype hand-held field test source consisting of a conventional microscope illuminator and chopper was fabricated. There was enough near-IR energy from the bulb to yield adequate detector signal even though the detector response was down in the near IR. Typical signal levels from the tester held 1 cm from the fiber input are shown in Figure 20.

3. Field Tests

From 14 May to 1 June 1979, the IR fiber receiver described in this report was used (in Grafenwohr, Germany) in field tests of a 10- μ m BIFF link. HRL personnel participated in the tests, which consisted of illuminating the receiver with a pair of TEA laser pulses at ranges out to 2.7 km. Both spatial coherence (measured by varying the fiber separation) and temporal coherence (measured by varying the delay between laser pulse pairs) of the received signals were recorded. Although the data reduction to be performed by NVEOL has not yet been completed, on-site observations show good performance out to the maximum range of 2.7 km.

The IR fiber performed flawlessly during the tests. The two fibers installed in the unit before shipment functioned throughout the tests. The back-up fiber cables supplied for the tests were not needed.

8854-14

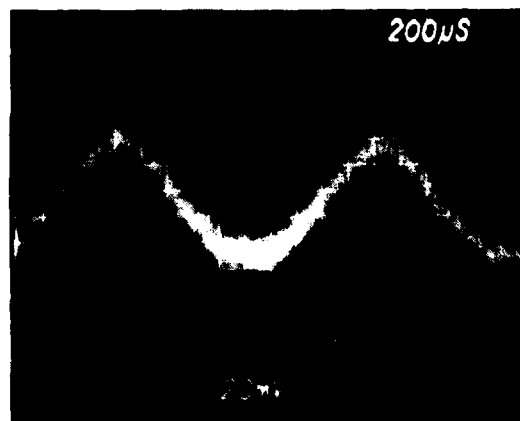
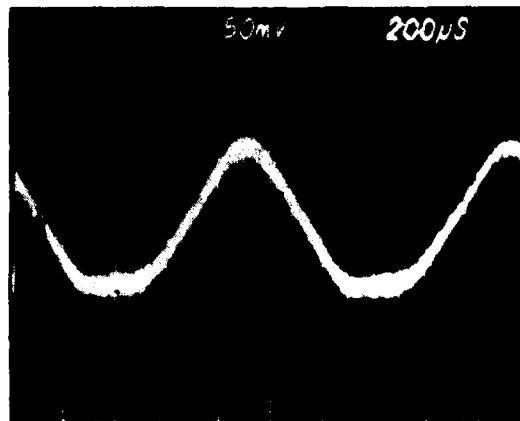


Figure 20. Response of HgCdTe detectors illuminated with visible light test source.

The LN_2 dewars, which had last been pumped out in mid-March, functioned perfectly without any additional pumpout in the field. These results are most encouraging in light of the field test conditions encountered. The receiver was subjected to violent vibrations in transportation to and from its remote site, which was a tank training area riddled with deep ruts, and the excessive dust (caused by armored vehicles) that was usually present might also have degraded the optics. The results obtained under such conditions show that IR fibers are not just a laboratory curiosity but can be used in tactical situations as well.

SECTION 3

FUTURE PLANS

The plans for the remainder of the contract are summarized below in terms of the individual tasks discussed in Section 2.

A. TASK 1 - FIBER FABRICATION

We will continue to emphasize the extrusion of KCl. High-temperature extrusion will be attempted on unlubricated billets of KCl. With our new heater assembly (to be installed within the next month), temperatures in excess of 600°C will be possible. Extrusion in this temperature range should show whether or not it is possible to produce smooth, glassy-type surfaces free from any contaminating lubricant. Low-temperature extrusions will involve the use of special lubricants to reduce the friction between the die and fiber during extrusion. These lubricants must be removable from the fiber after fabrication so that the attenuation is not affected.

B. TASK 2 - EVALUATION

Optical absorption measurements will continue on fibers and billets (as required). In addition to the 10.6- μ m insertion-loss measurements, fiber attenuation will be studied at 5.2, 3.8, and 2.8 μ m. Scattering measurements will also be emphasized. Light scattering in single- and poly-crystalline materials will be evaluated as a means of studying the effect of grain boundaries and surface irregularities on scattering losses.

C. TASK 3 - BIFF

No further work on this task is currently contemplated.

SECTION 4

PAPERS AND PRESENTATIONS

1. "Infrared Fiber Optical Materials," A. L. Gentile, M. Braunstein, D. A. Pinnow, J. A. Harrington, D. M. Henderson, L. M. Hobrock, J. Myer, R. C. Pastor, and R. R. Turk. Presented at Conference on Physics of Fiber Optics, June 19-23, 1978. University of Rhode Island, Kingston, R. I.

Manuscript submitted for publication in conference proceedings (Plenum Press).

2. "Infrared Fiber Optics", J. A. Harrington. Presented at 27th National IRIS, Materials Specialty Group, May 16, 1979, San Diego, CA.